Climatology and Composite Evolution of Flash Drought over Australia and Its Vegetation Impacts

HANH NGUYEN,[a] MATTHEW C. WHEELER,[a] JASON A. OTKIN,[b] THONG NGUYEN-HUY,[c] AND TIM COWAN[c,a]

[a] *Bureau of Meteorology, Melbourne, Victoria, Australia*
[b] *Space Science and Engineering Center, Cooperative Institute for Meteorological Satellite Studies, University of Wisconsin–Madison, Madison, Wisconsin*
[c] *Centre for Applied Climate Sciences, University of Southern Queensland, Toowoomba, Queensland, Australia*

(Manuscript received 10 February 2022, in final form 2 March 2023, accepted 8 March 2023)

ABSTRACT: This study describes flash drought (FD) inferred from the evaporative stress index (ESI) over Australia and its relationship to vegetation. During 1975–2020, FD occurrence ranges from less than 1 per decade in the central arid regions to 10 per decade toward the coasts. Although FD can occur in any season, its occurrence is more frequent in summer in the north, winter in the southern interior and southwest, and across a range of months in the far southeast and Tasmania. With a view toward real-time monitoring, FD "declaration" is defined as the date when the ESI declines to at least −1, i.e., drought conditions, after at least 2 weeks of rapid decline. Composite analysis shows that evaporative demand begins to increase about 5–6 weeks before declaration with an increase in solar radiation, while evapotranspiration initially increases with evaporative demand but then decreases in response to the soil moisture depletion. Solar radiation increases simultaneously with precipitation deficit, both reaching their peak around declaration. FD intensity peaks with soil moisture depletion, 2–3 weeks after declaration. The composite wind speed only shows a modest increase around declaration. The composite FD ends 4 weeks after rapid decreases in solar radiation and increases in precipitation. Satellite-derived vegetation health composites show pronounced decline in the nonforested regions, peaking about 4–8 weeks after FD declaration, followed by a recovery period lasting about 12 weeks after flash drought ends. The forest-dominated regions, however, are little impacted. Modeled pasture growth data show reduced values for up to 3 months after the declaration month covering the main agricultural areas of Australia.

SIGNIFICANCE STATEMENT: Flash drought describes a fast intensification or rapid development of drought conditions with potential severe impacts on agriculture and ecosystems. This study describes the climatology and typical evolution of flash drought over Australia for the period 1975–2020. An objective definition of flash drought, using high-resolution observational-based datasets, is proposed and its spatiotemporal variability is provided, as well as its relationship with vegetation health and pasture growth. This constitutes a guideline for understanding flash drought in Australia and its impacts on vegetation.

KEYWORDS: Australia; Drought; Extreme events; Climatology

1. Introduction

Flash drought is any type of drought that has undergone rapid intensification (Otkin et al. 2018a). In Australia, the term flash drought was first mentioned in the media in 2018 (Doyle 2018) with the quote "the speed with which the impacts are felt is the flash drought's defining feature." Importantly, this speed of flash drought development means that agricultural producers are often unable to successfully deploy their traditional drought coping mechanisms in preparation. Detailed case studies have examined flash drought events that occurred in subtropical eastern Australia in 2018 and 2019 (Nguyen et al. 2019, 2021), and southeast Australia in 2015 (Parker et al. 2021), showing the large impacts of these cases.

Despite the large impacts shown by the case studies, to date, limited work has been done on the climatology of flash drought over Australia. Parker et al. (2021) presented a climatological description of flash drought over Australia using four indices derived from the ECMWF Reanalysis v5 (ERA5; Hersbach et al. 2020), describing flash drought in terms of the proportion of days per pixel and pixels per season in drought. They found that flash drought can occur anywhere in Australia and that the area-mean percentage of days for which their definition of flash drought is satisfied varies from 5.2% to 7.9% depending on the index. A more recent study by Christian et al. (2021) on the global distribution of flash drought detected from the standardized evaporative stress ratio (SESR) derived from four reanalysis products including ERA5, considered both the flash (rapid intensification) and drought (reduction in evapotranspiration) characteristics. They reported that flash drought is most likely to occur in the tropics and subtropics, with northern Australia experiencing flash drought occurrence in 20%–30% of all years, and southeastern Australia in about 15% of years. Christian et al. (2021) further showed a marked seasonality in flash drought occurrence with a peak in March for southeastern Australia and in January for northern Australia. They also demonstrated a statistically significant increasing trend in flash drought spatial coverage over southeastern Australia but decreasing trend over northern Australia, consistent with the

Corresponding author: Hanh Nguyen, hanh.nguyen@bom.gov.au

DOI: 10.1175/JHM-D-22-0033.1

long-term trends of the evaporative stress index (ESI) used as a proxy for drought conditions in Nguyen et al. (2020).

Building on previous work and focusing on Australia, we offer a more detailed climatology of flash drought using high-resolution observation-based data optimized for Australia and available from 1975 onward. We characterize flash droughts through objective definition of their declaration date, duration, intensity, and end date, where the "declaration" date is defined to occur after at least 2 weeks of rapid intensification, i.e., after the initial "flash" (more details below). This characterization is performed using high spatiotemporal resolution (~5 km, daily) ESI analyses. The ESI is chosen as it has been shown to be a good indicator for flash droughts (Nguyen et al. 2019, 2021) and drought conditions over Australia (Nguyen et al. 2020). Nguyen et al. (2020) showed that the ESI is highly correlated to a composite drought index, which is a weighted combination of four percentile-ranked single variable drought indices comprising precipitation, rootzone soil moisture, evapotranspiration, and normalized difference vegetation index (NDVI), and can accurately capture agricultural droughts. Corroborating this, Parker et al. (2021) also found that the ESI provides a reasonable representation of flash drought variability and onset, when comparing with the standardized precipitation index, evaporative demand drought index, and soil moisture index. Recently, Osman et al. (2021) compared multiple index definitions of flash drought over the contiguous United States and concluded that while some notable flash drought events are well captured by all definitions, other events are sensitive to definition. Although we recognize that the choice of index and definition may impact the identified flash drought characteristics (Koster et al. 2019; Osman et al. 2021; Qing et al. 2022), we argue that the ESI is suitable as an index, especially for agriculture (see, e.g., Otkin et al. 2018a).

Here, the ESI is derived from observation-forced outputs from the Bureau of Meteorology's land surface landscape water balance model version 6 (AWRA-L v6). We will present a flash drought climatology for the 46-yr period from 1975 to 2020 and examine the processes that occur around the time of flash drought declaration and the potential impacts of flash drought on vegetation over Australia. The paper is organized as follows. Section 2 describes the data and methods used to characterize flash drought. Sections 3–5 present the flash drought climatology, the typical evolution of surface hydrometeorological variables during flash drought, and the response of vegetation and pasture growth to flash drought. The summary and discussion are given in section 6.

2. Data and methods

The ESI is the standardized anomaly of the evapotranspiration to potential evapotranspiration (ET/PET) ratio:

$$\mathrm{ESI} = \frac{r_{\mathrm{et}} - \overline{r_{\mathrm{et}}}}{\sigma(r_{\mathrm{et}})},$$

where r_{et} = ET/PET is the ET/PET ratio, $\overline{r_{\mathrm{et}}}$ is its climatology, and $\sigma(r_{\mathrm{et}})$ is its seasonally varying standard deviation over a baseline period. In a water-limited hydroclimate like most of Australia, ET is highly influenced by the availability of moisture in the soil, while PET measures the atmospheric evaporative demand and depends mainly on solar radiation, temperature, vapor pressure deficit, and wind. Therefore, the ratio ET/PET is a powerful tool to describe drought, with rapid declines in the ESI to suitably large negative values being indicative of flash drought.

In this work, both ET and PET are obtained from the AWRA-L v6 model (Frost et al. 2018). AWRA-L produces daily outputs on a 0.05° grid over Australia back to 1911. However, here we limit our study period to 1975–2020 due to the use of climatological winds in AWRA-L prior to 1975 rather than observed daily-varying winds. The ESI is calculated daily on the AWRA-L resolution over a 4-week running average window, with the last day of the window being the date we assign to it.

Additional quantities derived from the ESI are used to fully define flash drought, following the method described by Nguyen et al. (2021):

(i) The standardized change in the ESI over a 2-week interval (δESI), computed from the difference between the ESI at a given instance and 2 weeks prior (dESI) as

$$\delta\mathrm{ESI} = \frac{d\mathrm{ESI} - \overline{d\mathrm{ESI}}}{\sigma(d\mathrm{ESI})}.$$

(ii) Rapid change index (RCI); estimated for each grid point and set to 1 when δESI falls below the 20th percentile (p20), otherwise 0:

$$\mathrm{RCI} = \begin{cases} 1, & \delta\mathrm{ESI} \le \mathrm{p20} \\ 0, & \delta\mathrm{ESI} > \mathrm{p20} \end{cases}.$$

(iii) Flash drought index (FDI); this is set to 1 when RCI is 1 for a sequence of at least 2 weeks and ESI ≤ -1 at the end of the 2-week period. The 2-week sequence reflects the rapid intensification required for flash drought occurrence and the -1 threshold reflects the requirement for drought at the end of the intensification period. After the first instance of FDI = 1, the FDI remains at 1 in the following days if the ESI is equal or less than -1, otherwise it is set to zero.

In addition to the above criteria, we choose to include in this analysis only those occurrences when FDI equals 1 for a sequence of at least 4 consecutive weeks to eliminate shorter periods of drought-like conditions. Except for this last criterion, all other criteria above can be applied in real time, and we call the point at which FDI first equals 1 as the declaration date, as this is the first possible date at which a flash drought may be declared to be occurring in real time. We note that this declaration date comes at least 2 weeks after the start or onset of the flash component of the flash drought definition, and the intensification may continue beyond this date, as illustrated with examples below.

Figure 1 illustrates the identification steps as described above for three cases at different locations. For each case,

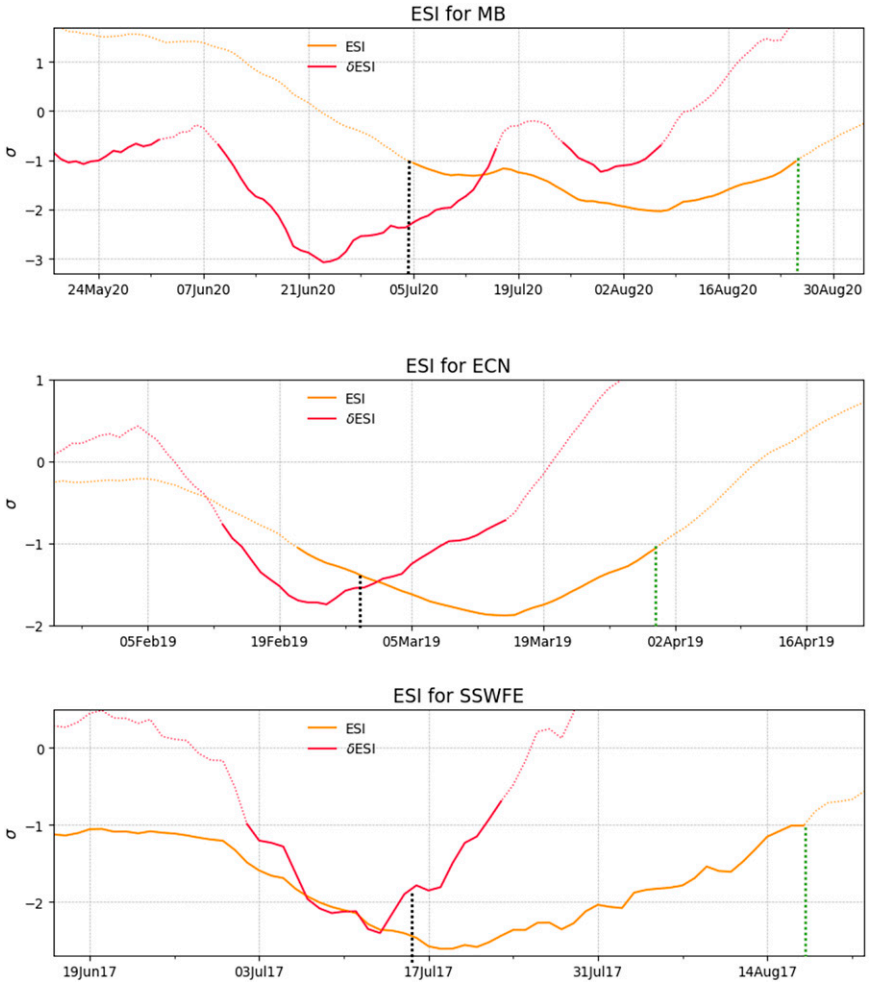

FIG. 1. Example time series of the ESI (yellow) with values below −1 shown as a thick line, and δESI (pink) with values below the 20th percentile in a thick line at three grid points (MB: 33.5°S, 144°E; ECN: 23.5°S, 149°E; SSWFE: 33.5°S, 116.5°E) where a flash drought event is identified. The vertical dotted lines indicate the flash drought declaration (black) and end (green) dates.

highlighted colored curves are used to indicate where RCI = 1, when δESI is below the 20th percentile, and where ESI ≤ −1, for a measure of drought. We further indicate with a vertical black dotted line the declaration date, that is, when FDI first equals 1. As defined above, this declaration can only occur when the RCI has been 1 for at least 2 weeks (i.e., the flash) and ESI ≤ −1 at the end of that 2-week period (i.e., the drought). We further define the end of an event as when the ESI next reaches above −1 corresponding to FDI = 0 (green dotted line), and it is only events that have their defined end at least 4 weeks after the declaration that are included in this analysis. These examples show that at the beginning of the rapid intensification (first instance RCI = 1), the ESI may sometimes be positive (Fig. 1, top panel), highlighting that evaporatively stressed conditions have not occurred yet, and that it may take several weeks before this state is met. In this case it took almost 4 weeks before ESI ≤ −1. On the other hand, the ESI may also sometimes already be negative prior to the rapid intensification (Fig. 1, bottom panel), indicating dry conditions are present before the intensification, and the declaration is made after the minimum 14 days from the start of that intensification. We verified that over the period of study and for all grid points over Australia, 44% of the flash drought events have their declaration date exactly 14 days after the onset of rapid intensification and the rest have it spread between 15 and 106 days (not shown). In this work we are concerned with the processes that occur in the lead up to and around the time of our defined declaration date, and as we will show (section 4), this declaration date sits on average several weeks after the onset of the rapid intensification, and several weeks before the peak intensity of the drought conditions.

In addition to the above definitions of flash drought declaration and end, we define the duration as the number of days

from the declaration to end, noting that this duration mostly includes only the "drought" component of the full "flash drought" period. We define the intensity as the averaged ESI over the duration of the event.

We note that the ESI used here has the same definition as the standardized evaporative stress ratio (SESR) as used by Christian et al. (2019, 2021). However, the subsequent method to detect flash drought in this study differs from the one adopted in Christian et al. (2019, 2021). While the term "ESI" was first introduced in the literature to refer to a product derived from satellite data (Anderson et al. 2013), here we choose to keep the term ESI instead of changing to the term SESR to remain consistent with our previous studies (Nguyen et al. 2019, 2020, 2021).

Time lag composite analysis is performed to establish the evolution of key hydrometeorological variables around the time of flash drought declaration. These variables are ET, PET, 1-m rootzone soil moisture (SM), precipitation, maximum temperature (Tmax), solar radiation, and 2-m wind speed. Precipitation, Tmax, solar radiation, and wind speed are from the Australian Gridded Climate Data (AGCD)/Australian Water Availability Project (AWAP) gridded product (Australian Bureau of Meteorology 2020) and are on the same spatiotemporal resolution as AWRA-L variables. The ET, PET, and SM variables are outputs of AWRA-L. Because the ESI is averaged over a 4-week running window, the same running average and standardization is applied to these variables prior to the time lag composite analysis. Noting that solar radiation, derived from satellite measurements, is available only from 1990 onward, analysis on this variable is done over the shorter period 1990–2020. The composite is performed at each grid point with reference to flash drought events, then averaged over specific regions such as the Natural Resource Management (NRM) clusters (https://www.climatechangeinaustralia.gov.au/en/projections-tools/regional-climate-change-explorer/sub-clusters/, last accessed January 2022) sharing similar hydroclimate features. The time lags used are every 7 days relative to the flash drought declaration or end date.

To assess the potential impacts of flash drought on vegetation, we investigate the relative evolution of vegetation health products from the NOAA Center for Satellite Applications and Research (STAR, https://www.star.nesdis.noaa.gov/smcd/emb/vci/VH/index.php, accessed August 2021). We use the vegetation health index (VHI) and noise-removed NDVI derived from radiances observed by the Advanced Very High Resolution Radiometer (AVHRR) satellites. These data have a spatial resolution of 4 km and temporal resolution of 7 days. Therefore, there are 52 fixed time steps per year, available from 1982 to 2020. Appreciating that the vegetation health products are on a weekly time scale, we compute the lag composite by taking all values closest to the declaration date to account for lag 0, then we calculate the lags at weekly intervals. This is also done on each grid point prior to averaging over the NRM clusters. These data are linearly interpolated to the ESI spatial resolution of 5 km prior to the composite computation.

Another product relevant to agriculture is pasture growth. Here we use the accumulated monthly pasture growth data from the AussieGRASS Environmental Calculator (Carter et al. 2000; DSITI 2015) to examine the relationship with flash drought. AussieGRASS is a modeling framework based on the Grass Production (GRASP) model (Rickert et al. 2000) that includes daily observed weather information such as precipitation, temperature, solar radiation, humidity, evaporation and vapor pressure deficit, soils, pasture type, tree cover, and stock numbers. The pasture growth output is produced monthly on the same horizontal resolution as AWRA-L, accumulated over a given month. Pasture growth represents the new plant material produced during the given month and is measured by the total standing dry matter, and is usually expressed in kilograms of dry matter per hectare (kg DM ha^{-1}). Model outputs are assessed and calibrated against in situ measurement over more than 100 sites across Australia (DSITI 2015). It is important to note the model caveats in the DSITI (2015) report, such as some growth limiting processes that are not well modeled including extreme or protracted droughts, or not simulated including floods and degradation processes. Monthly lag composite of pasture growth with reference to flash drought is computed, where lag 0 is the average of monthly values closest to the flash drought declaration date.

3. Flash drought climatology

Flash drought statistics over 1975–2020 for Australia are presented in Fig. 2. Here the frequency of occurrence is defined as the total number of flash drought events over the 46 years expressed in events per decade. The declaration month refers to the most frequent month in the climatology. The mean duration and intensity are the average values over the total number of flash droughts. The frequency of occurrence tends to be higher toward the coasts with up to 10 events per decade and lower occurrence of less than 1 per decade in the central arid regions. Seasonality of the most frequent declaration month is also apparent, showing a preferred occurrence in summer in the north, in winter in the southern interior and southwest, and a mixture of months around the far southeast and Tasmania. The mean duration, by our definition, varies between 28 and 120 days suggesting that flash droughts are a mostly subseasonal-to-seasonal climate phenomenon, although we note that this duration does not include the initial intensification period that lasts at least two weeks before our declaration date. The mean intensity represented by the ESI exhibits a similar spatial pattern as the frequency of occurrence, ranging from −1.01 in the central regions to −2.26 toward the coasts.

The seasonality of occurrence described above approximately coincides with the climatological maximum of precipitation in the north versus south of Australia. This suggests that flash droughts in Australia may be primarily associated with precipitation deficit during times of normally high precipitation. This seasonality is consistent with Koster et al. (2019), who found in the Northern Hemisphere that precipitation deficit is the main driver in reducing soil moisture and leading to flash droughts, while evaporative demand has secondary effects and/or only driving fewer flash droughts.

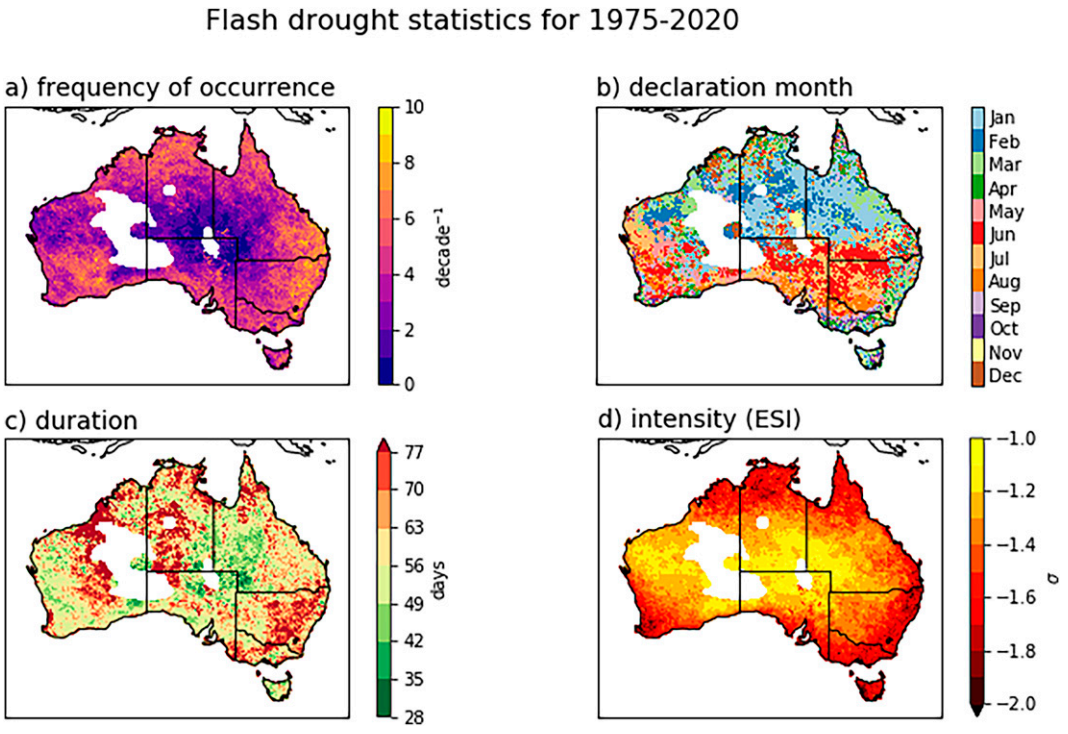

FIG. 2. Flash drought characteristics for Australia over the 1975–2020 period, derived from the ESI. (a) Frequency of occurrence (events per decade), (b) the most frequent declaration month, (c) mean duration (days), and (d) mean intensity as measured by the ESI.

Similarly, Parker et al. (2021) show that precipitation variability is a primary indicator of flash drought variability. We will consider the hydrometeorological drivers of flash drought in more detail below.

To capture further insight on flash drought occurrence, we investigate their statistics either area-averaged for the 13 NRM clusters or individually at 15 selected grid points. These NRM regions and selected points are shown in Fig. 3a. Note that the four points in the Monsoonal North East (NME) and West (MNW) regions correspond to locations of specific interest to the Northern Australia Climate Program (NACP[1]; Cobon et al. 2021). The monthly distribution of flash drought occurrence averaged for all grid points belonging to the 13 NRM clusters is shown in Fig. 3c. This gives further information on the annual distribution of occurrence, not just the most frequent month, as was shown in Fig. 2b. This distribution shows that some regions have more than one peak month and that there are some months in some regions with very few observed flash drought declarations (e.g., less than 2% of the total occurrences in December in SSWFE). There is also a clear latitudinal variation. In the Wet Tropics (WT), flash drought is most common in January, April, and December, and has its minimum in June during the climatological dry season. A similar seasonal cycle of flash drought occurrence is observed in the Monsoonal North (MNE and MNW) and East Coast North (ECN) regions, with the most flash drought declared in the summer to autumn months of December–April. Of all the regions, the East Coast South (ECS) has the most even distribution of occurrence through the year, while the Central Slopes (CS) has a slight maximum in June. Farther south in the Murray Basin (MB) and Southern Flatlands (SSWFE and SSWFW), there is a more prominent winter maximum, while in the Southern Slopes (SSVE, SSVW, SSTE, and SSTW) there is a transition back to a slight summer to autumn maximum.

Turning now to the all-season statistics for frequency, duration, and intensity, Fig. 4 shows the 5th, 50th, and 95th percentiles of each quantity as a distribution in each of the 13 NRM regions. The distributions show regional variability in terms of the frequency, with the lowest occurrence over the MNE and SSTW, and highest in the East Coast regions. The median value of flash drought duration varies little, unlike the 95th percentile. Flash drought duration also shows some regional variation but without any apparent link to variation in the frequency. Here, the ECS and SSTW regions have the highest flash drought intensity, while the CS has the lowest.

Figure 4 also shows the location in the regional distributions of the flash drought characteristics for the 15 selected grid points (grid locations shown in Fig. 3a). Generally, the selected grid point statistics are located within the distribution and near the median of their respective NRM clusters,

[1] NACP is a program aimed at helping the northern beef industry manage drought risk and climate variability.

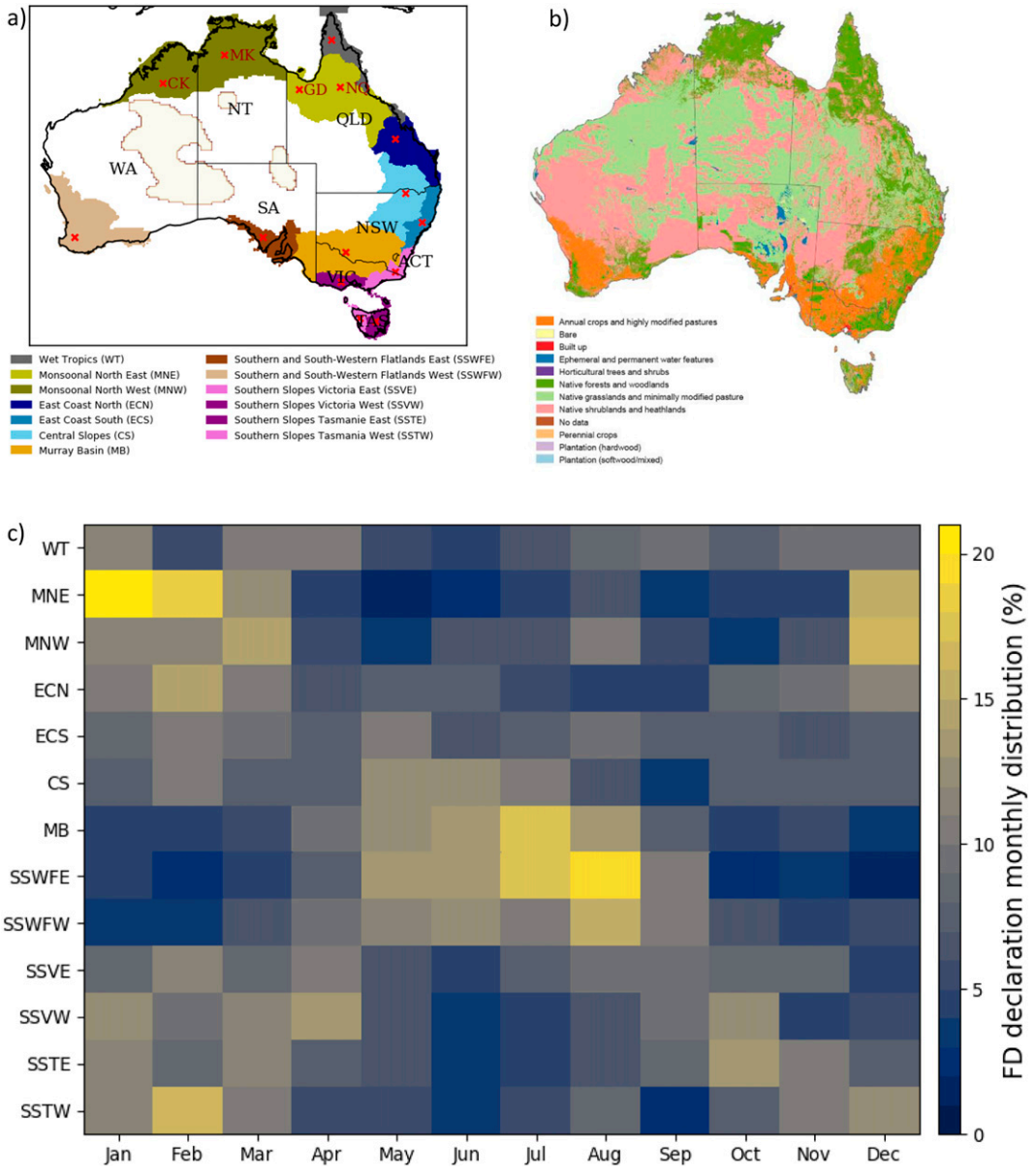

FIG. 3. (a) The 13 clusters of NRM regions taken from https://www.climatechangeinaustralia.gov.au/en/projections-tools/regional-climate-change-explorer/sub-clusters/ and 15 selected grid points within those clusters, 4 of which are locations of special interest to the NACP Climate Mates (https://www.nacp.org.au/outreach/climate_mates): Central Kimberley (CK), Mathison-Katherine (MK), Gregory Downs (GD), North Queensland (NQ). (b) Vegetation types across Australia taken from the Australian Bureau of Agricultural and Resource Economics and Sciences, Integrated Vegetation Cover dataset 2009 (https://soe.environment.gov.au/theme/land/topic/2016/vegetation-0). (c) The monthly distribution of flash drought declaration month averaged over the NRM clusters for the 1975–2020 period as a percentage of all months.

although with a notable exception of the frequency at the ECN site that sits outside of the 5th percentile.

Additional information at these selected grid points, such as the longest flash drought, the most intense flash drought, and the highest occurrence in a calendar year, is provided in Table 1. The frequency at these sites varies between 3.7 (Gregory Downs and ECN) and 7.2 (SSVE) events per decade. The most occurrences are two in a year at 10 of the sites and three at 5 sites (in the years 1982 for ECS, 1987 for SSVE, 1990 for Central Kimberly, 2002 for Mathison-Katherine, and in 2019 for SSTE). While the median duration at the selected grid points is between 50 (Mathison-Katherine) and 78 (SSWFW) days (Fig. 4), the longest flash drought is recorded as 445 days, with an intensity of −2.55 in 2019 at the ECS grid point

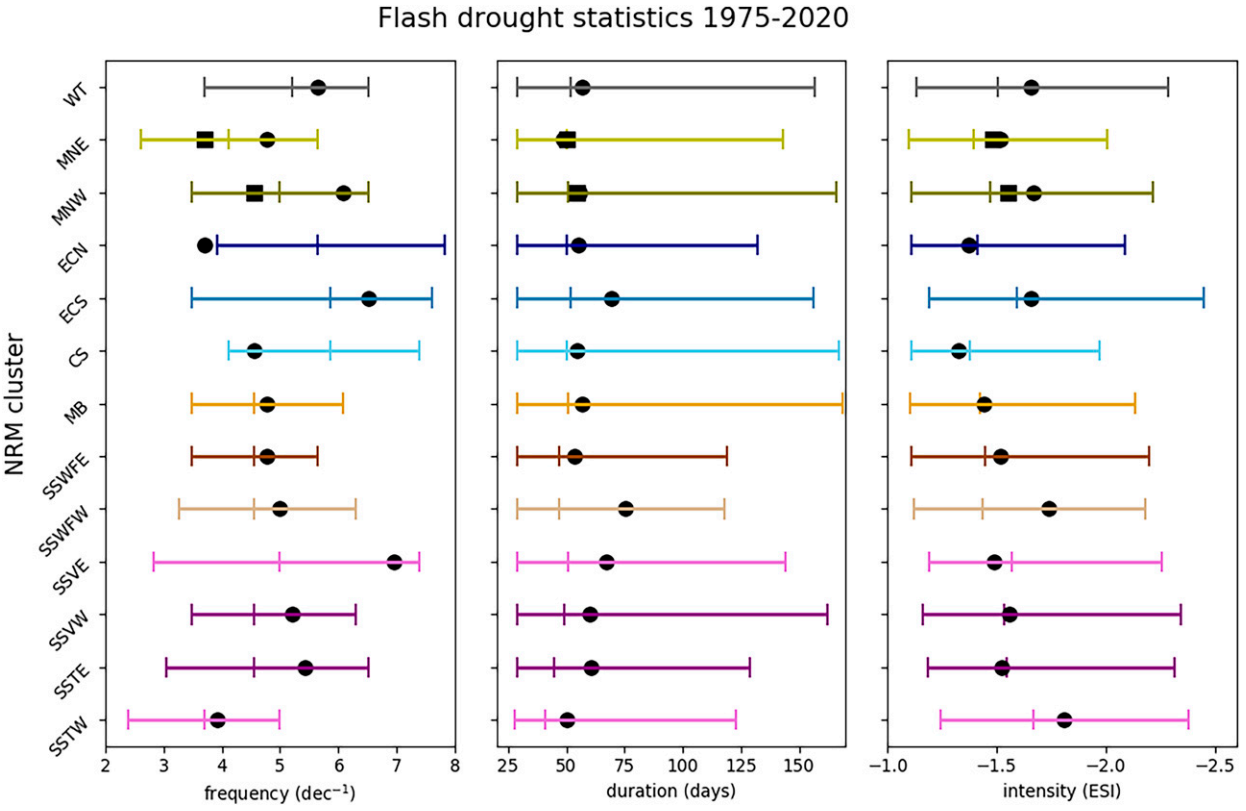

FIG. 4. Gridpoint flash drought characteristics for the 13 NRM clusters over all seasons of the 1975–2020 period: (left) frequency of occurrence (events per decade), (center) mean duration (days), and (right) mean intensity (ESI). The 5th, 50th, and 95th percentiles across all grid points are displayed for each NRM cluster, and the filled black dots are the selected gridpoint values at the locations indicated by a red cross in Fig. 3a. For the MNE and MNW clusters, the dots and squares represent the west and east locations, respectively.

(Table 1; see also Nguyen et al. 2021). Further, while the mean intensity varies between −1.35 at the CS site and −1.82 at the SSTW site (Fig. 4), the most intense flash drought recorded at any of the 15 selected grid points had an intensity of −2.79 at Mathison-Katherine in 1988 that lasted 53 days.

We now consider time series of flash drought at the 15 selected grid points versus a more conventional index of longer-term drought. Nguyen et al. (2020) demonstrated that the ESI can also be used as a robust conventional drought index for Australia, sharing similar characteristics with a monthly combined drought index (CDI), a composite of four single factor indices, and of relevance for agriculture. The conventional drought is defined to occur when the ESI drops below 0, with a minimum duration of 6 months, and terminates when the ESI flips back above 0 [see Nguyen et al. (2020) for more computational details]. When superimposing the conventional long droughts and flash droughts together in Fig. 5, we find that at any one grid point, flash drought can occur either as part of a conventional drought event or in isolation. However, there is a tendency for more flash droughts that last longer and are more intense during the major conventional drought events indicated in Nguyen et al. (2020) (e.g., the 1982/83 and 1991–95 El Niño–driven events, the 2001–09 Millennium Drought, and the 2013–15 and 2017–19 events).

4. Link with surface hydrometeorological variables

To get a better understanding of the processes that occur around flash drought declaration, time-lag composites of standardized anomalies of precipitation, solar radiation, maximum temperature, wind speed, soil moisture, ET, PET, and ESI are computed with respect to the flash drought declaration dates for each grid point, then averaged over the NRM region (Fig. 6a). Here lag day 0 corresponds to the declaration date. In all 13 NRM clusters, all variables except wind speed evolve in much the same way regardless of the region with the only readily apparent difference being their magnitudes.

Looking in more detail at the wind speed, its anomalies are generally weak ($\leq 0.5\sigma$) and inconsistent among the 13 clusters. In ECN, ECS, and SSVE, there is an increased wind speed starting about 3 weeks prior to the declaration, peaking 1–2 weeks after the declaration, then plateauing. In the other clusters, the wind speed displays less systematic behavior. This lack of a clear signal suggests that wind speed has little or no systematic role in flash drought across most of Australia and can be removed from generalized descriptions of flash drought.

TABLE 1. Flash drought statistics for the 15 selected grid points indicated in Fig. 3a for 1975–2020. Columns 2 and 3 indicate the intensity (I; unitless), duration (D; days), and declaration date of the longest event and most intense event, respectively. Column 4 indicates the highest number of occurrences in a calendar year, and the total number of occurrences during 1975–2020 with the year given in parentheses for those locations with three or more occurrences in that year. The most extreme values among the 15 locations are highlighted in bold font.

	Longest FD (I/D/declaration)	Most intense FD (I/D/declaration)	Highest occurrence in a year/total occurrences
Wet Tropics (WT)	−1.59/149/18 Aug 2016	−2.5/38/3 Apr 1986	2/26
Monsoonal North East—Gregory Downs (GD)	−1.56/111/17 Jan 1986	−1.95/66/1 Feb 1990	2/17
Monsoonal North East—North Queensland (NQ)	−1.11/79/10 Apr 1988	−1.87/66/6 Feb 1990	2/22
Monsoonal North West—M K (MK)	−1.8/166/20 Aug 2019	**−2.79/53/10 Mar 1988**	3 (2002)/28
Monsoonal North West—Central Kimberly (CK)	−1.74/120/26 Dec 1991	−2.44/51/29 Feb 1988	3 (1990)/21
East Coast North (ECN)	−1.37/163/19 Feb 1993	−1.85/42/26 Dec 2019	2/17
East Coast South (ECS)	**−2.55/445/9 May 2019**	−2.56/64/22 Dec 1980	3 (1982)/31
Central Slopes (CS)	−1.28/94/27 Feb 2005	−1.63/83/6 Jun 2018	2/21
Murray Basin (MB)	−1.42/157/11 Jul 2002	−2.24/58/11 Jun 1984	2/22
Southern and South-Western Flatlands East (SSWFE)	−1.9/150/10 Jul 2006	−2.17/59/13 Jun 2005	2/22
Southern and South-Western Flatlands West (SSWFW)	−1.9/375/3 Mar 1994	−2.65/67/14 Sep 2010	2/22
Southern Slopes Victoria East (SSVE)	−1.63/174/18 Feb 1986	−2.21/69/13 Aug 1994	**3 (1987)/33**
Southern Slopes Victoria West (SSVW)	−2.1/235/5 Aug 1982	−2.27/55/3 Jul 1984	2/24
Southern Slopes Tasmania East (SSTE)	−2.24/179/13 Apr 2002	−2.43/52/19 Apr 2016	3 (2019)/25
Southern Slopes Tasmania West (SSTW)	−1.85/115/7 Mar 1988	−2.44/62/3 Jan 2016	2/18

Compared to the wind speed, however, the other variables show much more systematic variation. In all regions the composite ESI undergoes a sharp drop from near zero about 3 weeks prior to the declaration to a minimum about 2 weeks after. ET tends to initially increase reaching a local maximum 4 weeks prior to the declaration before decreasing with a week delay compared to the ESI. This increase then decrease of the ET is like that shown by Jiang et al. (2022) for droughts in tropical South America, explained as evidence for a shift from an energy-limited regime to water-limited regime during the drought progression. The standardized magnitude of the ET is comparable to the ESI, except in Tasmania. In contrast, the PET tends to be flatter with a smaller amplitude (of about 1σ compared to ET anomalies $>1.6\sigma$) and reaches a maximum one week after flash drought declaration.

With all 13 NRM clusters sharing a similar composite evolution and to increase the robustness of the results, we further average the composites across all 13 clusters in Fig. 6b. In this composite, the solar radiation and precipitation are the first variables to show changes from about 5–6 weeks prior to declaration. With the expectation of solar radiation mainly controlling PET through its impact on temperature, the composites clearly show the coevolution between Tmax and PET peaking about a week after the solar radiation. For the water-related variables, soil moisture initially decreases in response to precipitation deficit but continues to decline, reaching its minimum 2 weeks after the precipitation minimum. This 2-week lag may be explained by the combined influence of precipitation deficit and increased temperature (and therefore PET) on soil moisture as has been suggested by Qing et al. (2022). After its initial increase, ET then decreases in response to soil moisture depletion and reaches its minimum a few days after the soil moisture.

While most previous studies have focused on the development and onset of flash droughts, little is known about their typical end. Case studies have shown that the ESI can quickly return to positive values following heavy precipitation, marking the transition from drought to above normal conditions (Otkin et al. 2019; Nguyen et al. 2021), but it is not known if this result can be generalized. Here we apply the time-lag composite with reference to the flash drought end dates to show the composite averaged over all 13 clusters in Fig. 6c. Here, flash drought is defined to end when ESI > -1, equivalent to when FDI switches back to 0. The composite shows that precipitation increases from its minimum 4 weeks before flash drought ends to positive anomalies about a week before. This increase in precipitation is about twice the rate as the decline in precipitation that occurs in the composite for declaration, somewhat confirming the case studies mentioned above. At the same time, solar radiation increases at a similar rate. Again, temperature and therefore PET decreases in direct response to solar radiation, while soil moisture and ET transition back to neutral with a delay of 2 weeks but also at a slower rate, taking about 5 weeks to transition from the minimum to neutral conditions. This delay in the ET recovery is somewhat like what has been observed in the Amazon by Jiang et al. (2022), who attributed the phenomenon in that region to feedback from drought-induced enhancement of forest mortality. Whether forest mortality is occurring and/or playing a role in Australia will be assessed in the next section.

5. Flash drought impacts on vegetation/pasture growth

The satellite-based NOAA STAR vegetation health products have been successfully used for a range of applications including food security prediction (Kogan et al. 2018, 2019), forecasting malaria (Nizamuddin et al. 2013), and drought monitoring (Kogan et al. 2017). Here, we examine the relationship between flash drought and VHI and NDVI for the NRM clusters. Weekly time-lag composites based on flash drought declaration are computed at each grid point then averaged over each

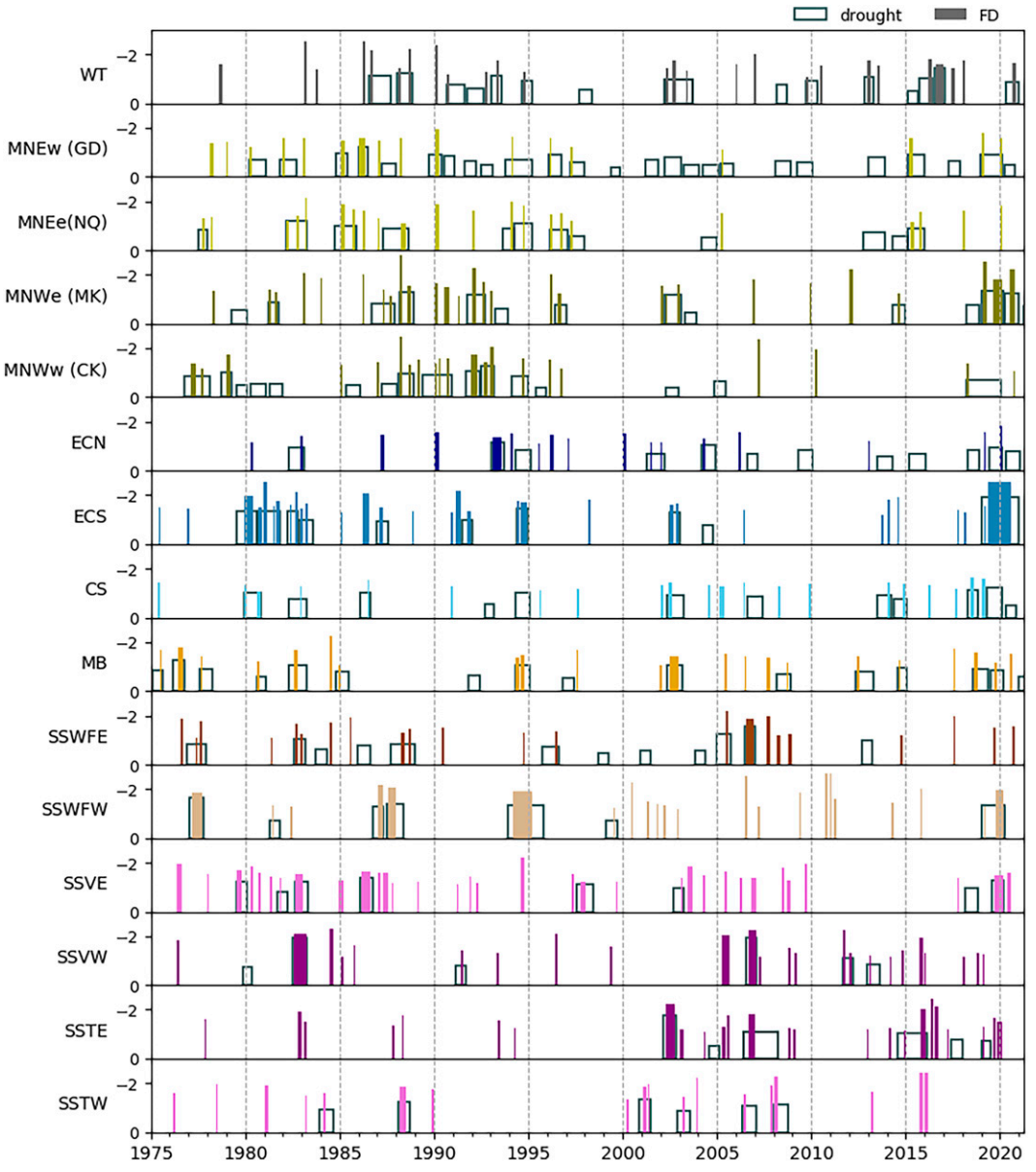

FIG. 5. Flash drought (filled bars) occurrences for the selected 15 gridpoint locations within the NRM clusters shown in Fig. 3a. The thickness of the bars indicates the flash drought duration, and the height of the bars represents the flash drought intensity. Conventional long drought events as defined in Nguyen et al. (2020) are superimposed (open bars). Note that the open bars here are different to those presented in Fig. 13 of Nguyen et al. (2020) as in that study the open bars were showing area averages.

of the 13 NRM clusters, as shown in Fig. 7. Of the 13 NRM clusters, four show little change in vegetation health relative to the declaration: the Wet Tropics (WT), the two in Tasmania (SSTE and SSTW), and the Southern Slopes Victoria East (SSVE). All remaining clusters exhibit a pronounced decline in both VHI and NDVI, reaching their minima about 5 and 7 weeks after flash drought declaration, respectively. We note the abrupt jump in the SSVE VHI composite at week 3. We are unsure why this occurs, but think it is more likely a data issue than something physical since such jumps are absent from the SSVE curves in Fig. 6.

The differing vegetation responses to flash drought shown in Fig. 7 might reflect the different types of dominant vegetation in the clusters. Indeed, Fig. 3b shows that the clusters with little VHI response are dominated by native forests and woodlands which tend to have much deeper roots than the vegetation of the other regions that are dominated by annual crops and pasture (Metcalfe and Bui 2017). For these deep-rooted vegetation types to be affected by a drought event, the drought duration would presumably need to be longer than the typical flash drought time scale to deplete the deeper soil

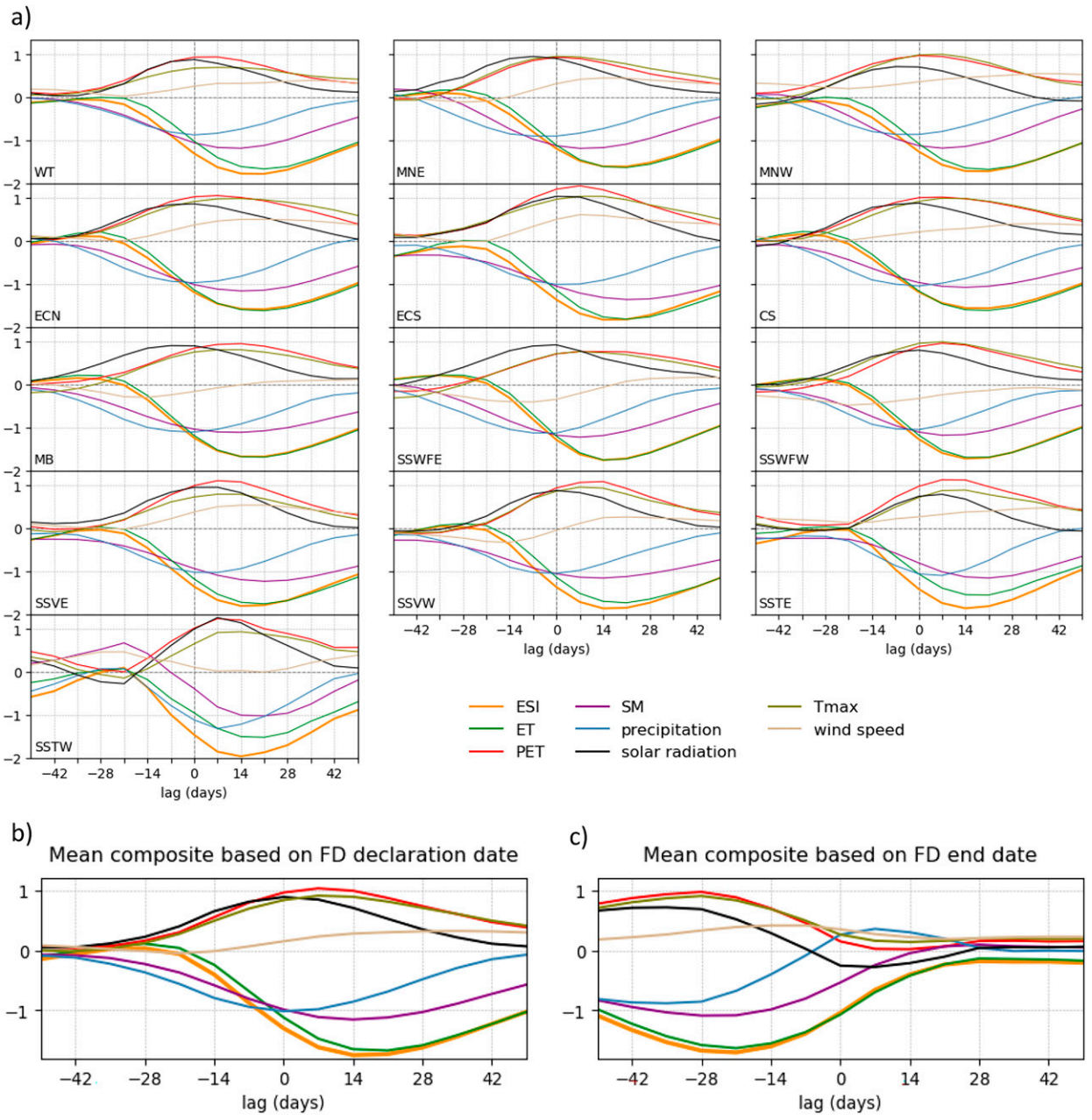

FIG. 6. (a) Lag composite, in increment of 7 days, with reference to the flash drought declaration date computed for individual grid point then averaged over each of the 13 NRM clusters indicated in Fig. 3a, with lag 0 day corresponding to the flash drought declaration date. On each panel are standardized anomalies of ESI, ET, PET, SM, precipitation, solar radiation, Tmax, and wind speed. The variables are averaged over a 4-week window and standardized by their daily climatological value prior to computing the composites. Time series were computed using all flash drought events from 1975 to 2020. (b) Mean composite with reference to the flash drought declaration date averaged over the 13 NRM clusters. (c) Mean composite with reference to the flash drought end date averaged over the 13 NRM clusters.

layers. Therefore, it is expected that longer-term drought would be more likely to affect the dominant vegetation in these woodland/forested regions than flash drought.

In section 4 we discussed the delay in ET recovery after the end of flash drought, which in other continents have been suggested to result from feedback related to forest mortality (Jiang et al. 2022). We further test the role of vegetation in Australia by computing the VHI and NDVI composite based on flash drought declaration and end dates, but separately for the forest-dominated clusters versus the rest (Fig. 8). Like in the composites of Fig. 7, it appears that the forest-dominated NRM clusters have little vegetation response, and this result also applies to flash drought end. This strongly suggests that unlike in the Amazonian droughts studied by Jiang et al. (2022), forest

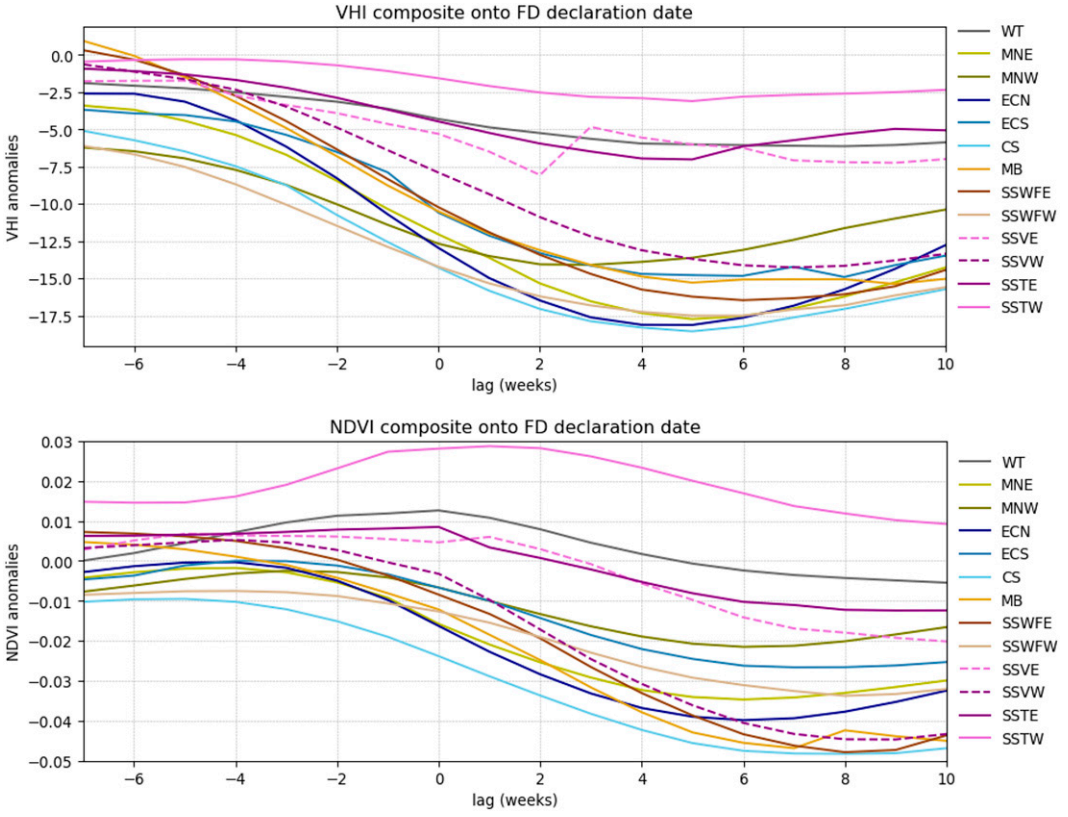

FIG. 7. Lag composite with reference to the flash drought declaration date computed at individual grid points then averaged over the 13 NRM clusters, with lag 0 day corresponding to the declaration date. The composite is done every 7 days. (top) Vegetation health index (VHI) and (bottom) noise-removed NDVI anomalies. The variables are averaged over a 4-week window prior to the composite computation.

mortality is playing little or no role in prolonging the negative ET anomalies beyond the end of flash droughts in Australia. Interestingly, however, the nonforest NRM clusters do show a very slow recovery for vegetation after flash drought end, not returning to the predrought state even 12 weeks after flash drought end. To what extent this slow vegetation recovery feeds back onto the ET is unknown, but given that the ET recovers from about 3 weeks after flash drought end (Fig. 6c) compared to more than 12 weeks for the vegetation, any feedback must be small.

For the forest-dominated NRM clusters, it is interesting to note that the mean NDVI composite, with reference to the declaration date, shows a slight increase (dashed orange curve in Fig. 8b), reaching a maximum at about the time of declaration before decreasing. This may be a sign that for forests, the initial stages of flash drought may actually promote forest productivity, likely due to the increased solar radiation, similar to what has been discussed for the Amazon by Jiang et al. (2022).

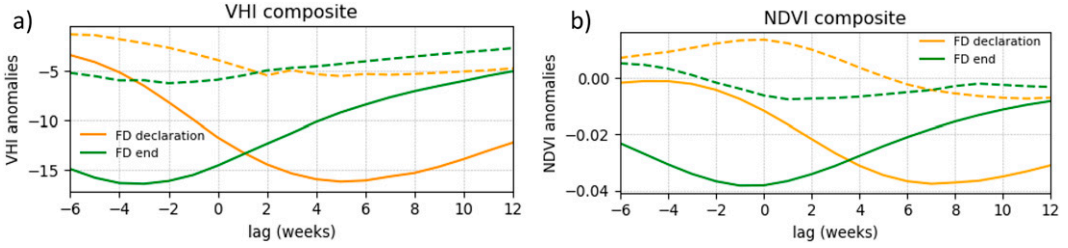

FIG. 8. Mean lag composite of (a) VHI and (b) NDVI with reference to the flash drought declaration (orange) and end (green) dates computed at individual grid points then averaged over the four forest-dominated NRM clusters (WT, SSVE, SSTE, and SSTW; dashed) vs the rest of the clusters (solid). Lag 0 day corresponds to the declaration or end date.

Accounting for the fact that the above vegetation health products include all types of vegetation and that one of the aims of this study is to assess whether flash drought specifically impacts the grazing industry in Australia (Cobon et al. 2021), we now examine the monthly evolution of modeled pasture growth relative to the flash drought declaration month at grid point scale. Time-lag composites of pasture growth (Fig. 9) show that in the month leading up to the declaration (lag −1 month), pasture growth anomalies are near neutral across almost all grid points. These neutral values are then mostly replaced by negative growth anomalies for lag months 0, 1, and 2 in large areas, with some improvement in month 3, giving the impression of a strong impact on pasture growth lasting several months.

Looking at Fig. 9 in more detail, small patches of negative anomalies are evident in scattered locations in the east at lag −1 month. This may be because of some possible mixing in temporal signals induced by the composite calculation with monthly pasture data. For instance, a flash drought declaration of 30 June would use May as the prior month, whereas if it had started a day later on 1 July, then June would be used as the prior month. This could cause a 1-month earlier shift in the pasture composite in some scattered locations that happen to have their declaration date near the beginning of the calendar month. This might also show the AussieGRASS model's limitations related to its caveats mentioned in section 2 where some growth limiting processes including droughts are not well modeled (DSITI 2015). Nevertheless, the map at lag month 0 is in stark contrast with lag month −1. At lag 0, there are large areas of strong negative anomalies of less than −200 kg DM ha^{-1}, which corresponds to about a 20% drop from the peak seasonal mean pasture growth value. These anomalies are seen for grid points across the north and east but also in the southwest, coinciding with co-occurring strong negative ESI anomalies (top panel of Fig. 9). Most of these negative pasture growth anomalies persist into lag month 2. However, the grid points in Tasmania, eastern Victoria, and far north Queensland show no or little changes in the modeled pasture growth which is consistent with the little change in VHI and NDVI in these regions (Fig. 7) and that these are predominantly forested regions (Fig. 3b). Three months after the declaration month, pasture growth returns toward normal conditions except for western Victoria and southern New South Wales, consistent with flash drought durations being typically longer in these regions (Fig. 2c). The 3-month time scale is also broadly consistent with the 12-week recovery of vegetation indicated in Fig. 8, although we note that since these are growth anomalies, the impacts are actually accumulated. These results clearly show the importance of flash drought for pasture growth over the main grazing lands of Australia.

6. Summary, further discussion, and concluding remarks

This study offers a detailed description of flash drought characteristics at a 5-km grid scale over the past 46 years detected from the ESI computed using observation-based high-resolution daily ET and PET from the Bureau's AWRA-L model version 6. The climatology highlights that although flash droughts can exist in any season, their occurrence is more frequent in summer in the north, winter in the southern interior and southwest, and more frequent across a broader range of months in the far southeast and Tasmania. The climatology also highlights that although they can occur anywhere in Australia, by our definition, they are more common away from the central arid regions. This reflects that rapid reductions in ESI to negative values are very difficult to achieve in regions that are normally very water limited. Further, for the flash droughts that were identified in the central arid regions, little impact on pasture growth was found (Fig. 9). Flash drought therefore appears to be mostly irrelevant for these regions for which very dry conditions are normal and periods of wetness and greenness are the exception.

Our result of fewer flash droughts in the arid center is consistent with that obtained by Parker et al. (2021) when using the standardized soil moisture index. It is, however, interesting to note that while Parker et al. (2021) also tested an ESI-based definition of flash drought, the frequency of occurrence inferred by their use of the ESI shows a much more even spread over Australia. But it is also important to note that their ESI was derived from the ERA5-Land global model reanalysis dataset which does not have the same optimization to Australian conditions, and use of Australian observational data, as that of AWRA-L. Seasonal correlation between the ESI computed from AWRA-L and ERA5-Land shows generally low correlations across Australia, with the highest values found in summer (not shown).

Composite evolution of the variables impacting the ESI prior to and after flash drought declaration shows that precipitation deficit, the main ingredient for any type of drought, is first noticeable about 5–6 weeks prior to the declaration. Coincident with the precipitation decline, clearer skies and increased solar radiation lead to warmer surface temperatures and increased PET. On the other hand, the soil moisture response to precipitation decline is delayed by about 2 weeks, hence ET only starts decreasing about 3 weeks prior to flash drought declaration; initially the ET has a slight increase, peaking 4 weeks before the declaration. This increase-then-decrease pattern highlights the transition from an energy-limited to water-limited regime (Pendergrass et al. 2020; Jiang et al. 2022). PET peaks 1 week after the declaration, while ET closely follows the ESI, reaching its minimum 3 weeks after the declaration. This suggests that although the PET increase due to increased solar radiation may play a more important role during the intensification period, the peak intensity of the flash drought is better determined by the low ET and soil moisture. Importantly, this composite evolution serves to validate the theoretical flash drought evolution presented in the schematic of Pendergrass et al. (2020, their Fig. 3) with observations-based data for the first time.

Another novel aspect of this research is the composite computed around flash drought end. Case studies have previously shown that flash drought end can be very rapid due to heavy precipitation events. The composite evolution somewhat confirmed this, showing the precipitation increase preceding flash

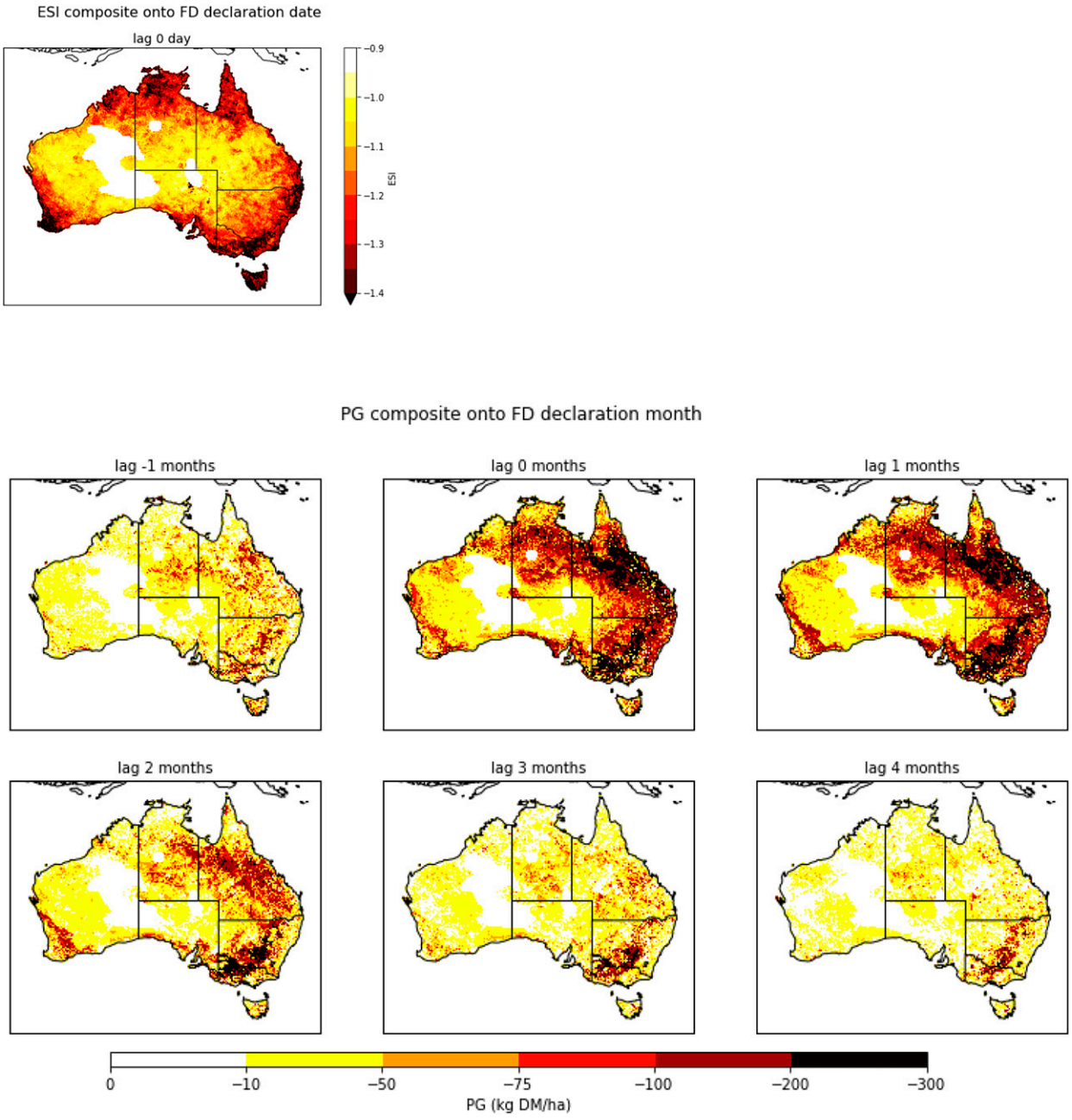

FIG. 9. Lag composite of pasture growth anomalies with reference to the flash drought declaration month on the grid point scale (in the bottom six panels). Note that because the pasture growth data are only available as monthly averages, the composite is done with respect to the declaration month. The ESI composite at lag 0 day (i.e., on the declaration day) is included in the top panel.

drought end to be about twice the rate as its decline preceding flash drought declaration.

Finally, we assessed the potential impact of flash drought on vegetation health. Weekly satellite-based NDVI and VHI products in the nonforested NRM regions exhibit a marked decline around flash drought declaration date with a minimum about 4–8 weeks later, depending upon the region, and a slower recovery of about 12 weeks. However, the forest-dominated NRM clusters did not show this change. Consistent with this, AussieGRASS monthly modeled pasture growth shows a reduction of about 20% of the climatological mean up to 3 months after flash drought declaration in the main agricultural and grazing areas.

The above results offer avenues for flash drought monitoring to be able to forewarn of impacts on vegetation health and pasture growth on the subseasonal time scale. For

example, knowing the typical flash drought evolution means that once a flash drought is declared in real time, grazing industries can then better manage their stock feed for the upcoming few weeks to months (Otkin et al. 2015, 2018b; Haigh et al. 2019). A more refined analysis using higher time resolution pasture growth (ideally daily) data could further inform the agricultural industry.

Preliminary work on daily outputs of modeled green cover and pasture biomass for experimental observing locations at the Alice Mulga SuperSite on Pine Hill cattle station, 200 km north of Alice Springs (22.28°S, 133.25°E) and the Wambiana grazing trial, 70 km southwest of Charters Towers (20.56°S, 146.11°E) (Owens et al. 2019), suggests that the ESI may potentially be useful as a predictor for these outputs with a lead time of 15 and 25 days, respectively. We plan to explore this in more detail, as more locations become available.

Acknowledgments. This study is funded by Meat and Livestock Australia, the Queensland Government through the Drought and Climate Adaptation Program, and the University of Southern Queensland through the Northern Australia Climate Program (NACP). We thank Jo Owens for her invaluable knowledge in the GRASP and AussieGRASS models and for her input on pasture growth data. We warmly thank Huqiang Zhang and David Jones as well as the three anonymous reviewers and the editor for their valuable comments that improved greatly the manuscript.

Data availability statement. This publication is supported by multiple datasets. Those openly available are at locations cited in the reference section. The others are obtained upon request and subject to license restrictions from a number of different sources cited in the reference section. Due to confidentiality agreements with the funding program, supporting data can only be made available to bona fide researchers subject to a nondisclosure agreement.

REFERENCES

Anderson, M. C., C. Hain, J. Otkin, X. Zhan, K. Mo, M. Svoboda, B. Wardlow, and A. Pimstein, 2013: An intercomparison of drought indicators based on thermal remote sensing and NLDAS-2 simulations with U.S. Drought Monitor classifications. *J. Hydrometeor.*, **14**, 1035–1056, https://doi.org/10.1175/JHM-D-12-0140.1.

Australian Bureau of Meteorology, 2020: Australian Gridded Climate Data (AGCD)/AWAP; v1.0.0 Snapshot (1900-01-01 to 2020-06-30). Australian Bureau of Meteorology, accessed 25 February 2022, https://doi.org/10.4227/166/5a8647d1c23e0.

Carter, J. O., W. B. Hall, K. D. Brook, G. M. McKeon, K. A. Day, and C. J. Paull, 2000: Aussie GRASS: Australian grassland and rangeland assessment by spatial simulation. *Applications of Seasonal Climate Forecasting in Agricultural and Natural Ecosystems*, G. L. Hammer, N. Nicholls, and C. Mitchell, Eds., Atmospheric and Oceanographic Sciences Library, Vol. 21, Springer, 329–349, https://doi.org/10.1007/978-94-015-9351-9_20.

Christian, J. I., J. B. Basara, J. A. Otkin, E. D. Hunt, R. A. Wakefield, P. X. Flanagan, and X. Xiao, 2019: A methodology for flash drought identification: Application of flash drought frequency across the United States. *J. Hydrometeor.*, **20**, 833–846, https://doi.org/10.1175/JHM-D-18-0198.1.

——, ——, E. D. Hunt, J. A. Otkin, J. C. Furtado, V. Mishra, X. Xiao, and R. M. Randall, 2021: Global distribution, trends, and drivers of flash drought occurrence. *Nat. Commun.*, **12**, 6330, https://doi.org/10.1038/s41467-021-26692-z.

Cobon, D., C. Jarvis, K. Reardon-Smith, L. Guillory, C. Pudmenzky, T. Nguyen-Huy, S. Mushtaq, and R. Stone, 2021: Northern Australia Climate Program: Supporting adaptation in rangeland grazing systems through more targeted climate forecasts, improved drought information and an innovative extension program. *Rangeland J.*, **43**, 87–100, https://doi.org/10.1071/RJ20074.

Doyle, K., 2018: What you need to know about droughts: Why they happen and how they are defined. *ABC News/Weather*, 1 August, https://abc.net.au/news/2018-08-01/what-you-need-to-know-about-droughts/10051956.

DSITI, 2015: AussieGRASS Environmental Calculator: User guide version 1.5. Department of Science, Information Technology and Innovation, Queensland Government, 41 pp., https://data.longpaddock.qld.gov.au/static/about/publications/pdf/agrass_user_guide.pdf.

Frost, A. J., A. Ramchurn, and A. Smith, 2018: The Australian Landscape Water Balance model (AWRA-L v6). Technical description of the Australian Water Resources Assessment Landscape model version 6. Bureau of Meteorology Tech. Rep., 58 pp., https://awo.bom.gov.au/assets/notes/publications/AWRALv6_Model_Description_Report.pdf.

Haigh, T. R., J. A. Otkin, A. Mucia, M. Hayes, and M. E. Burbach, 2019: Drought early warning and the timing of range manager's drought response. *Adv. Meteor.*, **2019**, 9461513, https://doi.org/10.1155/2019/9461513.

Hersbach, H., and Coauthors, 2020: The ERA5 global reanalysis. *Quart. J. Roy. Meteor. Soc.*, **146**, 1999–2049, https://doi.org/10.1002/qj.3803.

Jiang, Y., M. Yang, W. Liu, K. Mohammadi, and G. Wang, 2022: Eco-hydrological responses to recent droughts in tropical South America. *Environ. Res. Lett.*, **17**, 024037, https://doi.org/10.1088/1748-9326/ac507a.

Kogan, F., W. Guo, and W. Yang, 2017: SNPP/VIIRS vegetation health to assess 500 California drought. *Geomatics Nat. Hazards Risk*, **8**, 1383–1395, https://doi.org/10.1080/19475705.2017.1337654.

——, ——, ——, and S. Harlan, 2018: Space-based vegetation health for wheat yield modeling and prediction in Australia. *J. Appl. Remote Sens.*, **12**, 026002, https://doi.org/10.1117/1.JRS.12.026002.

——, ——, and ——, 2019: Drought and food security prediction from NOAA new generation of operational satellites. *Geomatics Nat. Hazards Risk*, **10**, 651–666, https://doi.org/10.1080/19475705.2018.1541257.

Koster, R. D., S. D. Schubert, H. Wang, S. P. Mahanama, and A. M. DeAngelis, 2019: Flash drought as captured by reanalysis data: Disentangling the contributions of precipitation deficit and excess evapotranspiration. *J. Hydrometeor.*, **20**, 1241–1258, https://doi.org/10.1175/JHM-D-18-0242.1.

Metcalfe, D. J., and E. N. Bui, 2017: Australia state of the environment 2016: Land. Independent rep. to the Australian Government Minister for the Environment and Energy, Australian Government Department of the Environment and Energy, 162 pp., https://doi.org/10.4226/94/58b6585f94911.

Nguyen, H., M. C. Wheeler, J. A. Otkin, T. Cowan, A. Frost, and R. Stone, 2019: Using the evaporative stress index to monitor

flash drought in Australia. *Environ. Res. Lett.*, **14**, 064016, https://doi.org/10.1088/1748-9326/ab2103.

——, J. A. Otkin, M. C. Wheeler, P. Hope, B. Trewin, and C. Pudmenzky, 2020: Climatology and variability of the evaporative stress index and its suitability as a tool to monitor Australian drought. *J. Hydrometeor.*, **21**, 2309–2324, https://doi.org/10.1175/JHM-D-20-0042.1.

——, M. C. Wheeler, H. H. Hendon, E.-P. Lim, and J. A. Otkin, 2021: The 2019 flash droughts in subtropical eastern Australia and their association with large-scale climate drivers. *Wea. Climate Extremes*, **32**, 100321, https://doi.org/10.1016/j.wace.2021.100321.

Nizamuddin, M., F. Kogan, R. Dhiman, W. Guo, and L. Roytman, 2013: Modeling and forecasting malaria in Tripura, India using NOAA/AVHRR-based vegetation health indices. *Int. J. Remote Sens. Appl.*, **3**, 108–116.

Osman, M., B. F. Zaitchik, H. S. Badr, J. I. Christian, T. Tadesse, J. A. Otkin, and M. C. Anderson, 2021: Flash drought onset over the contiguous United States: Sensitivity of inventories and trends to quantitative definitions. *Hydrol. Earth Syst. Sci.*, **25**, 565–581, https://doi.org/10.5194/hess-25-565-2021.

Otkin, J. A., M. Shafer, M. Svoboda, B. Wardlow, M. C. Anderson, C. Hain, and J. Basara, 2015: Facilitating the use of drought early warning information through interactions with agricultural stakeholders. *Bull. Amer. Meteor. Soc.*, **96**, 1073–1078, https://doi.org/10.1175/BAMS-D-14-00219.1.

——, M. Svoboda, E. D. Hunt, T. W. Ford, M. C. Anderson, C. Hain, and J. B. Basara, 2018a: Flash droughts: A review and assessment of the challenges imposed by rapid onset droughts in the United States. *Bull. Amer. Meteor. Soc.*, **99**, 911–919, https://doi.org/10.1175/BAMS-D-17-0149.1.

——, T. Haigh, A. Mucia, M. C. Anderson, and C. Hain, 2018b: Comparison of agricultural stakeholder survey results and drought monitoring datasets during the 2016 U.S. Northern Plains flash drought. *Wea. Climate Soc.*, **10**, 867–883, https://doi.org/10.1175/WCAS-D-18-0051.1.

——, Y. Zhong, E. D. Hunt, J. Basara, M. Svoboda, M. C. Anderson, and C. Hain, 2019: Assessing the evolution of soil moisture and vegetation conditions during a flash drought–flash recovery sequence over the south-central United States. *J. Hydrometeor.*, **20**, 549–562, https://doi.org/10.1175/JHM-D-18-0171.1.

Owens, J., J. Carter, G. Fraser, J. Cleverly, L. Hutley, and J. Barnetson, 2019: Improving evapotranspiration in pasture and native vegetation models using flux tower data, remote sensing and global optimisation. *23rd Int. Congress on Modelling and Simulation*, Canberra, Australian Capital Territory, Australia, Modelling and Simulation Society of Australia and New Zealand, 414–420, https://mssanz.org.au/modsim2019/C6/owens.pdf.

Parker, T., A. Gallant, M. Hobbins, and D. Hoffmann, 2021: Flash drought in Australia and its relationship to evaporative demand. *Environ. Res. Lett.*, **16**, 064033, https://doi.org/10.1088/1748-9326/abfe2c.

Pendergrass, A. G., and Coauthors, 2020: Flash droughts present a new challenge for subseasonal-to-seasonal prediction. *Nat. Climate Change*, **10**, 191–199, https://doi.org/10.1038/s41558-020-0709-0.

Qing, Y., S. Wang, B. C. Ancell, and Z.-L. Yang, 2022: Accelerating flash droughts induced by the joint influence of soil moisture depletion and atmospheric aridity. *Nat. Commun.*, **13**, 1139, https://doi.org/10.1038/s41467-022-28752-4.

Rickert, K. G., J. W. Stuth, and G. M. McKeon, 2000: Modelling pasture and animal production. *Field and Laboratory Methods for Grassland and Animal Production Research*, L.'t Mannetje and R. M. Jones, Eds., CABI Publishing, 29–66.